

Discrimination of parametrizations for nuclear effects in neutrino scattering through comparisons of low (~ 700 MeV) and medium (~ 3 GeV) energy cross-section data

J. Grange,^{1,*} C. Juszczak,² J. Sobczyk,² and G. P. Zeller³

¹*University of Florida, Gainesville, Florida 32611, USA*

²*Institute of Theoretical Physics, Wrocław University, Wrocław, Poland*

³*Fermi National Accelerator Laboratory, Batavia, Illinois 60510, USA*

(Received 23 November 2013; published 22 April 2014)

High-quality charged current quasielastic scattering data have recently been reported for both muon neutrinos and antineutrinos from several accelerator-based neutrino experiments. Measurements from MiniBooNE were the first to indicate that more complex nuclear effects, now thought to be the result of nucleon pair correlations, may contribute to neutrino quasielastic samples at a much higher significance than previously assumed. These findings are now being tested by MINER ν A and other contemporary neutrino experiments. Presented here is a comparison of data from MiniBooNE and MINER ν A to a few example parametrizations of these nuclear effects. It has been demonstrated that such effects may bias future measurements of neutrino oscillation parameters, and so this issue continues to press the neutrino community. A comparison of data over a large range of neutrino energies is one approach to exploring the extent to which such nucleon correlations may influence our understanding and subsequent modeling of neutrino quasielastic scattering.

DOI: [10.1103/PhysRevD.89.073018](https://doi.org/10.1103/PhysRevD.89.073018)

PACS numbers: 14.60.Lm, 14.60.Pq, 14.60.St

Charged current quasielastic scattering (CCQE, $\nu_l + N \rightarrow l + N'$) is the dominant interaction channel in many neutrino oscillation measurements. In practice, the assumed simple multiplicity and topology of such processes allow for the recovery of the incident neutrino energy (an essential quantity in neutrino oscillation fits) using only measurement of the outgoing charged lepton. Assuming background processes can be reliably subtracted with adequate precision, such CCQE samples then become an attractive channel through which to extract oscillation parameters because the sole reliance on lepton kinematics avoids experimental complications associated with the need to explicitly reconstruct final state nucleons.

Recently, there has been mounting evidence to suggest that such CCQE processes may not be as simple as originally thought, particularly when scattering off nuclear targets [1]. The presence of correlated nucleon pairs in the nuclear environment may alter both the magnitude and kinematics of these interactions at a significant level. Resultant enhancements have been previously observed in transverse electron-nucleus data [2], but the role such effects play is only now being appreciated in the context of neutrino-nucleus scattering, in large part motivated by the MiniBooNE data [3,4].

Of course, it is important to get the physics right. The complex nuclear environment can have a potentially large impact on the determination of neutrino energy, (anti)

neutrino rates, and nucleon emission in neutrino oscillation analyses [5–9]. Additionally, some amount of model dependence enters the cross-section data through the necessary reliance (to some degree) upon an event generator for the purpose of background prediction and subtraction. Hence, much attention has been devoted to this topic in recent years. While the theoretical and experimental understanding of this issue is still taking shape, most neutrino experiments do not currently include a complete implementation of nuclear effects (including nucleon correlations) in their simulations. Lacking this, confrontation of the experimental data and leading models have often been limited to comparisons of the absolute cross section as a function of neutrino energy, E_ν , and hence suffer from model dependences inherent in extracting E_ν from the data. High statistics information from MiniBooNE has recently changed this and allowed detailed comparison of nuclear models to flux-averaged double differential distributions of the observed muon kinematics, available for the first time for both neutrino and antineutrino quasielastic scattering on carbon [3,4]. Furthermore, the full angular coverage of the final state muon offered by the spherically symmetric detector allows a unique test of the transverse enhancement expected due to nucleon pair correlations (such effects are expected to be largest for backwards-scattered muons relative to the incoming neutrino beam).

More recently, MINER ν A has reported measurements of the flux-averaged differential cross section, $d\sigma/dQ_{QE}^2$, for both neutrino and antineutrino quasielastic scattering also

*Present address: Argonne National Laboratory, Argonne, IL 60439, USA.

on a carbon-based target [10,11]. The analysis of the MINER ν A data further includes an exploitation of its fine-grained calorimetry to scrutinize hadronic activity near the quasielastic interaction vertex. Like the earlier MiniBooNE findings, the results suggest the presence of nuclear effects not included in widely used relativistic Fermi gas (RFG) [12] models which assume independent (and not correlated) nucleons in the nucleus. To facilitate a more direct comparison of the MiniBooNE and MINER ν A data, we present a recasting of the MiniBooNE experimental data in the same form as recently reported by MINER ν A [13].

Here, the exercise of producing normalized ratios in Q_{QE}^2 with respect to the nominal RFG model, as presented by MINER ν A, is repeated with the MiniBooNE neutrino and antineutrino quasielastic data. In this case, Q_{QE}^2 refers to the squared four-momentum transfer obtained using only reconstructed muon kinematics and assuming quasielastic scattering with a single target nucleon at rest,

$$E_{\nu}^{QE} = \frac{2(M'_n)E_{\mu} - ((M'_n)^2 + m_{\mu}^2 - M_p^2)}{2 \cdot [(M'_n) - E_{\mu} + \sqrt{E_{\mu}^2 - m_{\mu}^2} \cos \theta_{\mu}]}, \quad (1)$$

$$Q_{QE}^2 = -m_{\mu}^2 + 2E_{\nu}^{QE}(E_{\mu} - \sqrt{E_{\mu}^2 - m_{\mu}^2} \cos \theta_{\mu}), \quad (2)$$

where $E_{\mu} = T_{\mu} + m_{\mu}$ is the total muon energy and M_n, M_p, m_{μ} are the neutron, proton, and muon masses. The adjusted neutron mass, $M'_n = M_n - E_B$, depends on the separation energy in carbon, E_B , which is set to 34 (30) MeV for neutrino (antineutrino) scattering. Note that the Q_{QE}^2 formula explicitly assumes one-body QE interactions. While this assumption may be faulty, the comparison is well justified because the prediction also assumes the same condition. Therefore, we are able to compare exactly the same observable quantity and learn from the level of consistency. The deviation from true Q^2 is present in the experimental data due to nuclear effects and the inclusion of two body current contributions are implemented into the prediction. Divergences between the prediction and data show that Monte Carlo models are not perfect, but the comparison remains meaningful.

The results, along with the bare Q_{QE}^2 distributions used to produce the shape comparison, are presented for neutrinos in Fig. 1 and for antineutrinos in Fig. 2. In following which was reported by MINER ν A [10,11,13], a comparison is shown for two example alternatives: increasing the axial mass parameter, M_A , in the RFG model and including a parametrization of the transverse enhancement seen in electron-nucleus scattering. Both have been motivated by the MiniBooNE observations and are shown to provide viable descriptions of this data. The value for M_A is chosen from spectral fits to the MiniBooNE CCQE events [3] while electron scattering data on heavy nuclei provide the

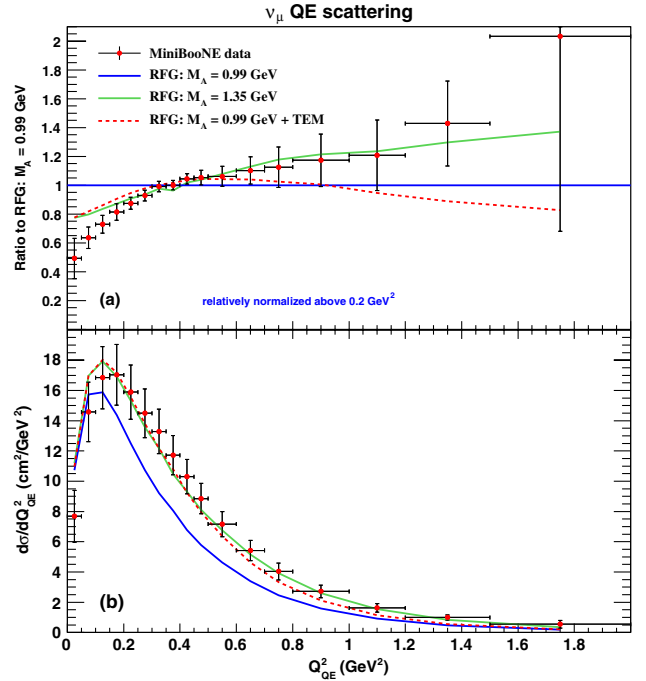


FIG. 1 (color online). The shape (a) and scale (b) of ν_{μ} MiniBooNE Q_{QE}^2 data compared to parametrizations of the RFG presented in the same form as MINER ν A data in recent publications [10,11,13]. Appropriate to each comparison, shape-only uncertainties accompany the data in (a), while total uncertainties are shown in (b). Within these experimental uncertainties, in the MiniBooNE energy range the effect of treating nuclear effects with an increase in the axial mass is largely consistent with the TEM description both in shape and in scale. Note that Pauli blocking has not been tuned in the models shown here, and so the agreement in the low Q_{QE}^2 region is somewhat worse compared to the tuned distributions shown in Refs. [3] and [4].

formulation of the Transverse Enhancement Model (TEM). In this implementation, the TEM specifically modifies the magnetic form factor for bound nucleons to achieve simultaneous agreement both with a wide range of electron scattering data and the early neutrino cross-section measurements on deuterium [14]. In the absence of a full nuclear physics description in neutrino event generators, such parametrizations can be a helpful tool for testing the gross features of such contributions and comparing data sets.

As for all models based on the impulse approximation, precision is not expected from the RFG in the region of small Q^2 [15]. For this reason, we focus on the higher Q^2 data and normalize the distributions presented here using the region $Q_{QE}^2 > 0.2 \text{ GeV}^2$. This excludes the most uncertain region of momentum transfer, $q < 450 \text{ MeV}$. The inclusion of RPA effects increases the accuracy of predictions in this region, and *is not* included in the models presented here. The ratios of the various distributions are executed after requiring the area of each differential cross

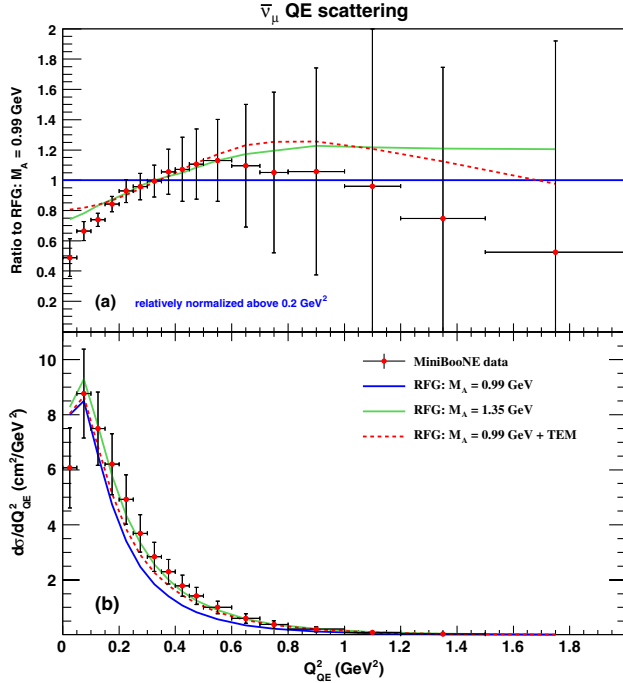


FIG. 2 (color online). The same distributions described in Fig. 1, but for $\bar{\nu}_\mu$. Note that, as is also the case for ν_μ , the $\bar{\nu}_\mu$ data appears simultaneously consistent with an increase in the axial mass and the introduction of the TEM.

section above 0.2 GeV^2 to match the cross-section strength in the same region of the the nominal RFG model with $M_A = 0.99 \text{ GeV}$. Apart from the focus on $Q_{QE}^2 > 0.2 \text{ GeV}^2$, the philosophy of these shape comparisons is identical to that of the MINERVA analyses.

To mitigate possible misinterpretations of these results due to the use of different neutrino interaction generators, the parametrizations of nuclear effects shown here are provided by the same NuWro neutrino event generator [16] as used in the published MINERVA results.

Both increases to the axial mass and the inclusion of transverse enhancement effects have been suggested as options to describe the MiniBooNE data. As seen in Figs. 1 and 2, in general these adjustments seem to perform equally well. There seems to be some mild tension at high Q_{QE}^2 between the TEM and the MiniBooNE ν_μ data; this has also been observed in comparisons of the model-independent double-differential distribution [17]. Because the inclusion of enhancements to the transverse current and increasing the axial mass can lead to similar results in the kinematic region accessed by the MiniBooNE flux, it can be difficult to disentangle their contributions. Future high-precision neutrino scattering experiments sensitive to this region such as MicroBooNE [18], NO ν A [19] and T2 K [20] may be able to provide a more discriminatory test of high momentum transfer interactions. Note that the MINERVA requirement of matching muons in the downstream calorimeter in order to recover the charge and momentum imposes an

effective Q^2 cut on the analysis sample. It may be possible to extend the kinematic range accessed by implementing the kinds of techniques described in Refs. [4,21].

When confronting these MiniBooNE plots with the similar version from MINERVA [13], the benefit of comparing data sets across very different neutrino energy ranges is immediately apparent. While the changes associated with an increase in the axial mass and the inclusion of transverse enhancement effects (according to the TEM) have very similar effects at low MiniBooNE energies ($0.4 < E_\nu < 2 \text{ GeV}$), the differences are much larger for higher MINERVA energies ($1.5 < E_\nu < 10 \text{ GeV}$) where the two effects start to pull apart. In the case of MINERVA, a large increase in M_A is not supported by the data and the TEM is more strongly favored [13]. Separating such nuclear effects from changes to the axial-vector form factor is important given that the two choices have very different implications for the interpretation of neutrino oscillation data.

The recent reports of the MINERVA and MiniBooNE CCQE data significantly extend the experimental knowledge of neutrino and antineutrino interactions on carbon nuclei. This robust collection of data offers an opportunity to directly test parametrizations of nuclear effects with neutrinos and antineutrinos across energy regimes crucial for current and next-generation oscillation experiments.

It will be interesting to repeat similar cross-comparisons with more sophisticated nuclear models such as microscopic calculations of multi-nucleon knock-out mechanisms [22,23]. An issue common to many such models is that they are reliable for the region of four-momentum transfer dominantly accessed by the MiniBooNE neutrino flux but not for the MINERVA flux [24]. Moreover, implementation of such models in Monte Carlo simulation requires the consistent inclusion of RPA effects, which leads to a considerably more complicated simulation scheme compared to present designs. We emphasize again that the model parameterizations compared to the MiniBooNE data in Figs. 1, 2 and the MINERVA data in Refs. [10] and [11] are limited in scope. While more realistic prescriptions are becoming available in the literature, the somewhat naive models discussed here are likely to see continued use in neutrino experiments. For this reason, their success in describing historical data sets is important to track and may be used to identify which features perform well in the context of the neutrino energies and kinematic regions accessed by unique experiments.

It will be with the sorts of high-resolution observations of both leptonic and hadronic activity in CCQE-like interactions presented by MiniBooNE and MINERVA, along with model-independent comparisons such as those presented here, that the neutrino interaction community will arrive at a definitive resolution to the size and kinematics of these important nuclear effects and what remaining role the axial-vector form factor plays. New data and improved

analyses from the MiniBooNE, MINER ν A, SciBooNE [25], MicroBooNE [18], ArgoNeuT [26], ICARUS [27], NOMAD [28], and the near detectors of the T2 K [20], NO ν A [19], and MINOS [29] experiments are expected to play vital roles in this campaign. Meanwhile, the continued aggressive theoretical progress and anticipated integration into neutrino generators used by experiments will be

invaluable towards understanding the fundamental basis for these interactions.

ACKNOWLEDGMENTS

C. J. and J. T. S. were partially supported by Grant No. 4574/PB/IFT/12 (UMO-2011/01/M/ST2/02578).

-
- [1] H. Gallagher, G. Garvey, and G. P. Zeller, *Annu. Rev. Nucl. Part. Sci.* **61**, 355 (2011).
- [2] J. Carlson, J. Jourdan, R. Schiavilla, and I. Sick, *Phys. Rev. C* **65**, 024002 (2002).
- [3] A. A. Aguilar-Arevalo *et al.* (MiniBooNE Collaboration), *Phys. Rev. D* **81**, 092005 (2010).
- [4] A. A. Aguilar-Arevalo *et al.* (MiniBooNE Collaboration), *Phys. Rev. D* **88**, 032001 (2013).
- [5] D. Meloni, *J. Phys. Conf. Ser.* **408**, 012024 (2013).
- [6] D. Meloni and M. Martini, *Phys. Lett. B* **716**, 186 (2012).
- [7] P. Coloma, P. Huber, C. M. Jen, and C. Mariani, [arXiv:1311.4506](https://arxiv.org/abs/1311.4506).
- [8] M. Martini, M. Ericson, and G. Chanfray, *Phys. Rev. D* **85**, 093012 (2012).
- [9] O. Lalakulich and U. Mosel, *Phys. Rev. C* **86**, 054606 (2012).
- [10] G. A. Fiorentini *et al.* (MINER ν A Collaboration), *Phys. Rev. Lett.* **111**, 022502 (2013).
- [11] L. Fields *et al.* (MINER ν A Collaboration), *Phys. Rev. Lett.* **111**, 022501 (2013).
- [12] R. A. Smith and E. J. Moniz, *Nucl. Phys. B* **43**, 605 (1972); **B101**, 547(E) (1975).
- [13] D. Schmitz (MINER ν A Collaboration), http://theory.fnal.gov/jetp/talks/Schmitz_WandC_MinervaCCQE_2013_05_10.pdf
- [14] A. Bodek, H. Budd, and M. E. Christy, *Eur. Phys. J. C* **71**, 1726 (2011).
- [15] A. Ankowski, O. Benhar, and N. Farina, *Phys. Rev. D* **82**, 013002 (2010).
- [16] T. Golan, C. Juszczak, and J. Sobczyk, *Phys. Rev. C* **86**, 015505 (2012).
- [17] J. T. Sobczyk, *Eur. Phys. J. C* **72**, 1850 (2012).
- [18] M. Soderberg (MicroBooNE Collaboration), *AIP Conf. Proc.* **1189**, 83 (2009).
- [19] D. S. Ayres *et al.* (NO ν A Collaboration), Report No. FER-MILAB-DESIGN-2007-01.
- [20] K. Abe *et al.* (T2K Collaboration), *Phys. Rev. D* **88**, 032002 (2013).
- [21] A. A. Aguilar-Arevalo *et al.* (MiniBooNE Collaboration), *Phys. Rev. D* **84**, 072005 (2011).
- [22] M. Martini, M. Ericson, G. Chanfray, and J. Marteau, *Phys. Rev. C* **80**, 065501 (2009).
- [23] J. Nieves, I. R. Simo, and M. J. V. Vacas, *Phys. Rev. C* **83**, 045501 (2011).
- [24] R. Gran, J. Nieves, F. Sanchez, and M. J. V. Vacas, *Phys. Rev. D* **88**, 113007 (2013).
- [25] Y. Nakajima *et al.* (SciBooNE Collaboration), *Phys. Rev. D* **83**, 012005 (2011).
- [26] C. Anderson *et al.* (ArgoNeuT Collaboration), *Phys. Rev. Lett.* **108**, 161802 (2012).
- [27] S. Amoroso *et al.* (ICARUS Collaboration), *Eur. Phys. J. C* **33**, 233 (2004).
- [28] V. Lyubushkin *et al.* (NOMAD Collaboration), *Eur. Phys. J. C* **63**, 355 (2009).
- [29] P. Adamson *et al.* (MINOS Collaboration), *Phys. Rev. D* **81**, 072002 (2010).